Neutron-deficient superheavy nuclei obtained in the ^{240}Pu + ^{48}Ca reaction

V. K. Utyonkov,[1,*] N. T. Brewer,[2] Yu. Ts. Oganessian,[1] K. P. Rykaczewski,[2] F. Sh. Abdullin,[1] S. N. Dmitriev,[1] R. K. Grzywacz,[2,3] M. G. Itkis,[1] K. Miernik,[2,4] A. N. Polyakov,[1] J. B. Roberto,[2] R. N. Sagaidak,[1] I. V. Shirokovsky,[1] M. V. Shumeiko,[1] Yu. S. Tsyganov,[1] A. A. Voinov,[1] V. G. Subbotin,[1] A. M. Sukhov,[1] A. V. Karpov,[1] A. G. Popeko,[1] A. V. Sabel'nikov,[1] A. I. Svirikhin,[1] G. K. Vostokin,[1] J. H. Hamilton,[5] N. D. Kovrizhnykh,[1] L. Schlattauer,[1,6] M. A. Stoyer,[7] Z. Gan,[8] W. X. Huang,[8] and L. Ma[8]

[1] *Joint Institute for Nuclear Research, RU-141980 Dubna, Russian Federation*
[2] *Oak Ridge National Laboratory, Oak Ridge, Tennessee 37831, USA*
[3] *Department of Physics and Astronomy, University of Tennessee, Knoxville, Tennessee 37996, USA*
[4] *Faculty of Physics, University of Warsaw, PL-02-093 Warsaw, Poland*
[5] *Department of Physics and Astronomy, Vanderbilt University, Nashville, Tennessee 37235, USA*
[6] *Faculty of Science, Palacký University, CZ-77147 Olomouc, Czech Republic*
[7] *Lawrence Livermore National Laboratory, Livermore, California 94551, USA*
[8] *Institute of Modern Physics, Chinese Academy of Sciences, Lanzhou 730000, China*

(Received 8 November 2017; published 30 January 2018)

We present new results from investigations of the ^{240}Pu + ^{48}Ca reaction at a projectile energy of 250 MeV. Three new decay chains of ^{285}Fl were detected with decay properties mostly consistent with those measured in earlier studies. An additional chain was observed where the nuclei may decay through energy levels different from those of the other six chains registered so far. The cross section of the ^{240}Pu(^{48}Ca,3n)^{285}Fl reaction was measured to be $0.58^{+0.60}_{-0.33}$ pb, which is a factor of about 4–5 lower than that measured in the previous experiment at 245 MeV beam energy [V. K. Utyonkov *et al.*, Phys. Rev. C **92**, 034609 (2015).], consistent with expectations. The origin of an additional chain consisting of a recoil, α particle, and fission event is analyzed. The assignment of 25 short-lived SF events observed in this experiment is also discussed.

DOI: 10.1103/PhysRevC.97.014320

I. INTRODUCTION

In this paper, we present the results of experiments aimed at the study of neutron-deficient Fl isotopes produced in the ^{240}Pu + ^{48}Ca reaction and of their descendants. Synthesis of neutron-deficient nuclei and the study of the properties of superheavy nuclei (SHN) in a wider range of number of neutrons could help to clarify the stabilizing effect of the experimentally established neutron shell closure at $N = 162$ and the one predicted at $N = 184$. During sequential α decays of Fl nuclei, having neutron numbers $N = 170-175$, descendant nuclei are formed, which are located closer to the $N = 162$ shell and even cross it in some decay sequences; thus, the stability of such nuclei is governed largely by the influence of this shell. The decay path involving nuclei with different neutron numbers may cause changes in structure that can manifest itself in the α-particle energy spectra and decay times. In addition, α-decay chains of the odd-N nucleus ^{283}Fl, the product of the 5n-evaporation channel of the studied reaction, could reach the domain of the known nuclei at $N \approx 162$, connecting the region of SHN to the nuclear mainland.

Of particular interest is the study of even-even nuclei whose decay properties, especially the probability of spontaneous fission (SF), are not distorted by the effect of the odd nucleon. The results of the first experiment involving the ^{240}Pu + ^{48}Ca reaction were published recently [1]. In Ref. [1], two events consisting of recoil (R) followed by spontaneous fission with relatively high energy release and with a half-life $T_{1/2} = 2.8$ ms were observed at the 250-MeV ^{48}Ca bombarding energy and tentatively assigned to ^{284}Fl. Two additional R-SF events registered with lower SF energy values might also originate from ^{284}Fl, however, their assignment to ^{240,242,244mf}Am fission isomers cannot be excluded. With the observed lifetimes of these events and the partial α-decay half-life estimated from extrapolation of α-decay energy (Q_α) systematics for Fl isotopes (e.g., Fig. 6 in Ref. [1]), and the relationship between T_α and Q_α, we could expect an α-decay branch of about 20% for ^{284}Fl. Observation of this decay mode would be important for final identification of the even-even isotope ^{284}Fl through its characteristic α-decay energy. In addition, the registration of its descendant, ^{280}Cn, that presumably undergoes spontaneous fission, would be important for tracing the properties of SHN in the $N \approx 168$–170 region of nuclei that exhibit the lowest stability against spontaneous fission. For ^{280}Cn ($N = 168$) a further decrease of $T_{\rm SF}$ is predicted as observed for neighboring Cn isotopes with decreasing N, but not as much as in neighboring isotopes ^{282,284}Cn (see Ref. [2] and Fig. 5 in Ref. [1]). Experimental verification of this prediction could shed light on stability of neutron-deficient isotopes of Fl, Cn, and other nuclei in this region.

*utyonkov@jinr.ru

Therefore, the main goal of this study was the synthesis of even-even ^{284}Fl with ^{48}Ca energy of 250 MeV and potential observation of its α decay, followed by decay of ^{280}Cn. In addition, one might expect production of ^{285}Fl at this projectile energy; this could give additional evidence of observation of the $3n$-evaporation channel by measuring the corresponding excitation function. Production of a new lighter Fl isotope, ^{283}Fl, at this beam energy seems to be less probable but cannot be completely excluded as well.

II. EXPERIMENT

The experiments were performed employing the Dubna Gas-Filled Recoil Separator (DGFRS) and using ^{48}Ca beams accelerated at the U400 cyclotron of the Flerov Laboratory of Nuclear Reactions, JINR. The maximum beam intensity of ^{48}Ca ions was 1.1 particle μA. The beam energy was measured with a systematic uncertainty of 1 MeV by a time-of-flight system. In this experiment, we used the same ^{240}Pu target as in Ref. [1]. The target material was provided by Oak Ridge National Laboratory (ORNL) (enrichment 98.97%, impurities of other Pu isotopes: 0.77% ^{239}Pu, 0.09% ^{241}Pu, and 0.17% ^{242}Pu) and JINR (enrichment 88.9%, impurities of other Pu isotopes: 7.7% ^{239}Pu, 1.4% ^{241}Pu, and 2.0% ^{242}Pu, according to later measurements). The average thickness of the target for ^{240}Pu was 0.39 ± 0.04 mg/cm^2 for the mixed ORNL/JINR target material combined in the ratio 1/5. The material was electrodeposited as PuO_2 oxide onto 0.72 mg/cm^2 Ti foils. The laboratory-frame beam energy in the middle of the target layer was about 250 MeV. Taking into account the energy spread of the incident cyclotron beam, the small variation of the beam energy during irradiation, and the energy losses in the target, we calculated the resulting ^{288}Fl compound nuclei (CN) to have an excitation energy range of 40.4–45.2 MeV (with use of mass tables [3,4]), close to that used in the second experiment with ^{240}Pu at $E_{\rm lab} = 250$ MeV in Ref. [1]. The total beam dose of ^{48}Ca particles was about 1.4×10^{19}.

Other experimental conditions, including the separator settings, detection system, electronics, and method of calibration of the detectors, were the same as in Ref. [1]. The transmission efficiency of DGFRS for $Z = 114$ evaporation residues (ER) was estimated to be 35 ± 5%. The volume of the separator was filled by hydrogen at a pressure of about 130 Pa. This volume is separated from the detection system by a 0.2 mg/cm^2 Mylar foil. After separation from ^{48}Ca beam ions, scattered particles, and transfer-reaction products, the recoils passed through a time-of-flight (TOF) system, that consisted of two multiwire proportional counters (MWPCs) placed in pentane at a pressure of about 200 Pa and generated signals proportional to the energy losses (ΔE) of recoils in the counters and TOF signals, and were finally implanted in the detector. Facing the incoming recoils is a 48-mm-high by 128-mm-wide 0.3-mm-thick double-sided silicon strip detector (DSSD) manufactured by Micron Semiconductor, Ltd. (model BB-17) with 1-mm-wide strips, 48 on the front side and 128 on the back side, providing high position resolution for recoil-correlated decay sequences and thus reducing potential random events. The detection efficiency of the implantation DSSD, for α particles with $E_\alpha \approx$ 10 MeV emitted from the implanted nuclei, was estimated to be about 52%. This detector was surrounded by an array of six single Si detectors (MICRON model MSX-7200) each 0.5-mm-thick with an active area of 65 mm (along the DSSD edge) by 120 mm (perpendicular to the DSSD surface). The inclusion of the side detectors, as measured for ^{217}Th α activity produced in a calibration reaction $^{\rm nat}$Yb + ^{48}Ca, increases the position-averaged detection efficiency for full-energy α particles from the decays of implanted nuclei to 85%. The DSSD was backed by a single Si-veto detector (MICRON MSX-62), of 0.5 mm thickness and 48 mm by 128 mm active size matching the respective DSSD area. It was used for the detection and rejection of signals from, e.g., high-energy charged particles (α, protons, etc.), which are produced in the reactions of projectiles with the DGFRS media and can pass through the separator without being detected by the ΔE and TOF system but can be recorded simultaneously in the DSSD and veto counters. The signals from all the detectors were processed by using linear MESYTEC preamplifiers. This Si-detector array was designed, assembled, commissioned offline, and provided by ORNL.

The output signals from the preamplifiers were split into two branches. One of these branches was processed with analog electronics and used to facilitate a low-background detection scheme for the nuclei to be investigated, similar to that used in Ref. [1]. This detection scheme allows the beam to be switched off after the detection of an ER-like signal followed by an α-like signal; provided the latter one is registered by the focal-plane detector with full energy. Both signals should occur in the same front and back strips of the focal plane detector within preset energy intervals expected for implantation and decay of the parent and daughter nuclei ^{284,285}Fl–^{277}Ds. Such a detection scheme provides registration of sequential decays of descendant nuclides with very low background. The second branch of split preamplifier signals was processed using a digital electronics system based on XIA Pixie-16 modules provided by ORNL (see Ref. [1] for more details).

Digital processing of DSSD signals allowed setting relatively low energy thresholds, of about 170 keV for the 48-mm-long front strips and about 430 keV for the 128-mm-long back strips. The full width at half maximum (FWHM) energy resolution of the implantation detector was 25–53 keV for back strips (54–87 keV for front strips), while the summed signals recorded by the side and implantation detectors had an energy resolution of 175–417 keV; the resolution progressively degraded after experiments with ^{240}Pu [1] and $^{249-251}$Cf [5] performed with the same side detectors. In the ^{206}Pb(^{48}Ca,$2n$)^{252}No calibration experiments, 61% of the SF events of ^{252}No were detected as two coincident fragments in the focal and side detectors, with an average measured total energy release $E_{\rm SF} = 167$ MeV (5 MeV lower than in Ref. [1]) and a FWHM of SF energy distribution $w = 35$ MeV. In addition, a long-lived SF activity remained in the same detectors after the experiment with a target containing $^{249-252}$Cf isotopes [5]. These nuclei can be assigned to recoiled target isotopes of ^{250,252}Cf with $E_{\rm SF} = 152$ MeV and $w = 31$ MeV. The average counting rates of SF events with $E_{\rm SF} > 80$ MeV and $E_{\rm SF} > 130$ MeV were about 32 and 21 per day, respectively. For the nuclides in the decay chains of Fl isotopes we expect minimum energies of fission fragments of 130 and 160 MeV for the fragments registered by the focal-plane detector only or simultaneously by the focal and side detectors, respectively.

III. RESULTS

In this experiment, performed at a ^{48}Ca beam energy of 250 MeV, we observed three decay chains of ^{285}Fl (Fig. 1). In the first experiment [1], carried out at the same ^{48}Ca energy but at a lower beam dose (4.7×10^{18}), only an upper cross section limit was determined for the $3n$ channel of the ^{240}Pu + ^{48}Ca reaction ($\leq$1.3 pb).

The first decay chain of ^{285}Fl was observed when the low-background detection scheme was not switched on. In the third chain, the first two α decays were registered by the focal and side detectors with low energy release in the focal detector. The decay of ^{277}Ds was registered by digital electronics in the neighboring back strips 63 and 64 with low energy release in strip 63 (0.69 MeV). In the analog electronics branch, this energy lies below threshold (1.57 MeV for back strip 63). This resulted in measuring a lower total α-particle energy on the back side and the beam was not switched off. The same occurred for the α particle of ^{285}Fl (back strips 68 and 69) in the second chain. Here only the α decay of ^{281}Cn stopped the beam and decays of ^{277}Ds, ^{273}Hs, and ^{269}Sg were detected during a 5-min beam-off period set in this experiment (the pause was not prolonged manually).

In this second chain, the full-energy α particle of ^{277}Ds was not found. Only three events were observed crossing the front strip 8 and back strips 68 and 69 while the beam was stopped by an ER-α_2 sequence; all of them are shown in Fig. 1. The probability of a random origin of an event with any energy in these strips within $\Delta t = 10$ ms is about 10^{-4} [6]. Thus, we assign the event registered by only the focal-plane detector, with energy of 0.6 MeV, to ^{277}Ds assuming that its α particle escaped the Si-box detectors. In the third chain, the SF event in front strip 21 and back strips 63 or 64 was observed about 1.8 h after the decay of ^{273}Hs (Fig. 1). Note, during the total 925-hour long experiment, only 39 SF events with $E_{SF} > 130$ MeV were found in front strip 21 and only one of them was detected in back strips 63 or 64 or simultaneously in both these strips (Fig. 1). Thus, we assign this event to ^{265}Rf because the probability of detection of a random SF event in these strips within $\Delta t = 2$ h was less than 3×10^{-3}. Between the decays of ^{273}Hs and ^{265}Rf, only one α particle with $E_\alpha > 7.8$ MeV was observed in the front strip 21 and back strips 63 or 64. In several parts of this experiment performed at the highest beam intensity during a total of about 40 h, we found 13 α-like events in the same strips and with $E_\alpha = 7.8$–8.8 MeV. The probability to detect one or more random α-like events within two hours from the decay time of ^{273}Hs is thus rather large, 0.48. However, the probability that a random event with $E_\alpha = 8.3 \pm 0.5$ MeV precedes the SF of ^{265}Rf ($\Delta t = 1$ min) is about 5×10^{-3} allowing us to assign this event to ^{269}Sg.

For calculation of the expected number of random ^{285}Fl-like decay chains, we first estimated probable energy range ΔE_{ER} for ERs of ^{285}Fl. We used the measured ER energies in the three chains shown in Fig. 1 and those from Ref. [1] for which the average E_{ER} value plus/minus three standard deviations result in $\Delta E_{ER} = 4.6$–15.1 MeV. This value is also in agreement with systematics of previously measured ER energies for nuclei

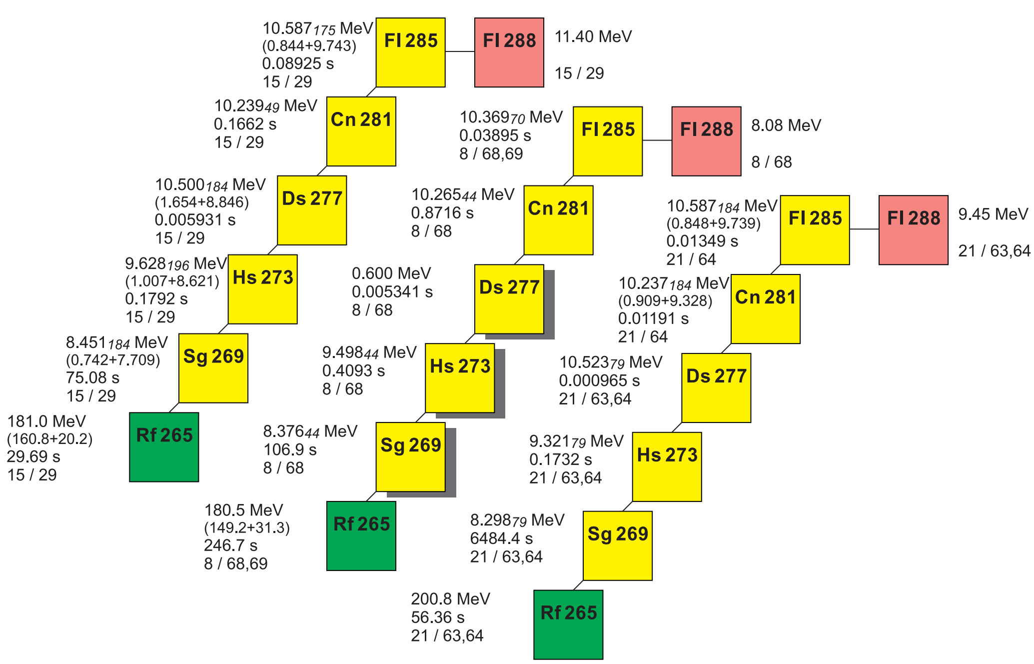

FIG. 1. Decay properties of ^{285}Fl and descendant nuclei observed in the ^{240}Pu + ^{48}Ca reaction. The decay chains listed in the text as events 1, 2, and 3 are shown from left to right. The top right rows for each chain show ER (in pink) energies and strip numbers (front and back). The left rows provide energies, time intervals between events and their strip numbers for α decay (in yellow) and SF (in green). Energies of summed signals are given in parentheses. Three events marked with a shadow were registered during the beam-off period. The FWHM α-particle energy errors are shown by smaller italic numbers. For events detected with full energy in one or two back strips the resolution corresponds to back or front strips, respectively.

synthesized in the U-Cf+^{48}Ca reactions as well as in various experiments with other projectiles carried out at DGFRS. During the 925-h ^{240}Pu + ^{48}Ca experiment when the beam was on the target, the total number of sequences consisting of ER-like events with $E_{ER} = 4.6-15.1$ MeV and α_1-like events with $E_\alpha = 10.4 \pm 0.5$ MeV detected within 0.5 s in the same front and back strips of the focal-plane detector was 543. The number of expected random ^{285}Fl-like decay chains was calculated by multiplying the 543 ER-α_1 chains (namely, numbers of chains in each of the back strips) by the corresponding probabilities of detection of different events (α and SF) in the same strips assuming their random distribution over the front strips. The total number of random chains was calculated as a summed value for all of the back strips. The probabilities of detection of events were calculated as numbers of events (α-like events with one energy interval $E_\alpha = 8.2$–10.7 MeV and SF events with $E_{SF} > 130$ MeV) in each of the back strips divided by the duration of experiment (925 h) and the number of the front strips (48) and multiplied by the time interval Δt. The last value was chosen as 10 s for decays of ^{281}Cn–^{273}Hs and 1000 s for ^{269}Sg and ^{265}Rf. Detection of events in chain 2 within the beam-off period was taken into account. For the first chain, the total number of random ^{285}Fl-like decay chains N_{ran} was about 2×10^{-14}. For the second chain, an escape event of ^{277}Ds was not taken into account, $N_{ran} < 2 \times 10^{-17}$. In the last case, the decays of ^{269}Sg and ^{265}Rf with lifetime of about 2 h were not taken into account as well, $N_{ran} < 4 \times 10^{-8}$. Thus, it is very unlikely that any of the three above decay chains of ^{285}Fl are due to random correlation of unrelated events.

In addition to the three decay chains of ^{285}Fl, one more chain was observed in this experiment. The ER-like signal with $E = 9.39$ MeV was followed in 12.21 s by an α particle with energies of 0.709 MeV and 8.804 MeV registered in the focal-plane and side detectors, respectively ($E_{tot} = 9.51 \pm 0.21$ MeV). In the next 0.0922 s, a fission event with $E =$ 195 MeV was detected by the focal (188 MeV) and side (7 MeV) detectors in the same front (38) and back (85) strips. No signals were observed between the ER-like event and the α particle in both these strips simultaneously. However, 17 low-energy signals ($E < 0.8$ MeV) were detected in the back strip 85 solely within this time interval; such signals could arise from an α particle escaping the focal detector. This chain is unlikely to originate from ^{285}Fl. Despite the fact that the energy of the α particle is comparable with that of ^{273}Hs, the ER-α time interval exceeds its lifetime by factor of 17, the probability of missing four α particles of ^{285}Fl to ^{277}Ds and ^{269}Sg in one chain is very low, and the decay time of 0.09 s is much lower compared to lifetimes of ^{269}Sg and ^{265}Rf. The decay properties of nuclei in this chain also contradict those expected for ^{284}Fl because the α-particle energies of the first three chain members ^{284}Fl–^{276}Ds should exceed the observed value of 9.5 MeV by about 1 MeV. The total number of such random chains was calculated similarly to that for ^{285}Fl. But because of the unknown origin of this chain, we applied extended energy intervals for the recoil (2.5–18 MeV) and α event (8–11 MeV); the time intervals were chosen to be 20 s and 1 s for α and SF events, respectively. Nevertheless, the total number of random recoil-α-SF chains is about 4×10^{-3}. The possible origin of this chain will be discussed in Sec. IV.

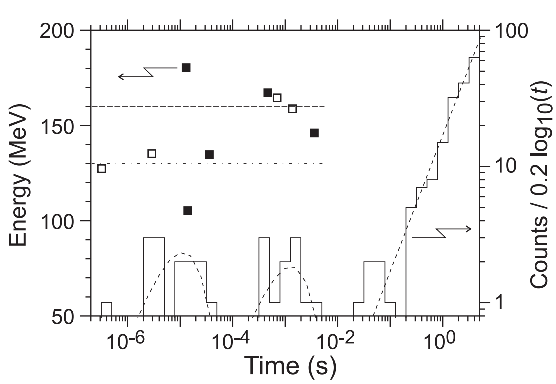

FIG. 2. Distribution of time intervals between SF events and all the preceding recoils (histogram, right scale). Short-dashed lines show exponential fits for decays with half-lives of about 10 μs and 1 ms and linear fit for random ER-like events. Energies of SF events following ER-like signals, which fit the interval expected for ERs of ^{284}Fl, are shown by solid and open squares for SF events registered by the focal and side detectors or solely by the focal detector, respectively (left scale, their expected lower energy limits are shown by long-dashed and dash-dotted lines, respectively).

TABLE I. Decay properties of short-lived SF nuclei observed in the ^{240}Pu + ^{48}Ca reaction. The ER energy, decay time, and SF energy are shown for each chain. The ER and/or SF energies, which fall within intervals expected for implantation and fission of ^{284}Fl are given in bold.

Event No	E_{ER} (MeV) - decay time (μs)-E_{SF} (MeV)[a]	E_{ER} (MeV) - decay time (μs)-E_{SF} (MeV)[b]	E_{ER} (MeV) - decay time (μs)-E_{SF} (MeV)[c]
	~1-ms activity	~1-ms activity	~10-μs activity
1	**6.29**-1376-**159**	**5.43**-3571-146[d]	1.25-23-131[d]
2	**8.55**-703-**165**	39.40-2370-**184**	**11.06**-13-**180**[d]
3	**12.02**-468-**167**[d]	3.41-1026-136[d]	2.05-28-129
4		4.11-813-**140**	**12.64**-36-135[d]
5		17.50-363-**181**	**7.03**-14-105[d]
6		3.81-1359-**169**[d]	2.62-12-**169**[d]
7		1.66-1933-113	2.89-12-139[d]
8		3.31-337-**133**	**8.90**-0.32-127
9			16.84-4.87-**141**
10			**14.43**-2.88-**135**
11			4.50-4.2-130
12			1.46-2-92
13			3.43-2-106
14			1.29-5-99

[a]Chains with decay time of about 1 ms, which could originate from ^{284}Fl.
[b]Chains with decay time of about 1 ms, which could be assigned to ^{284}Fl with lower confidence.
[c]Chains with decay time of about 10 μs. The ER and/or SF energies of most of these events do not correspond to intervals expected for ^{284}Fl.
[d]Fission events registered by both the focal-plane and side detectors.

Finally, in this experiment, we observed 25 short-lived SF nuclei. Since observation of fission isomers produced in transfer reactions with ^{240}Pu is quite expected [1], their fission energies should be lower than those of the nuclei with $Z \geqslant 104$, and they can reach detectors with broad distribution of energies of recoils, we searched for R-SF sequences in the recoil-energy interval of 0.3–50 MeV followed by fission fragments with energies larger than 90 MeV.

The distribution (number of events versus time interval in double logarithmic scale) for all such sequences within a 5-s time interval is shown in Fig. 2. In total, 755 chains were found within R-SF time interval of 20 s; 607 SF events were preceded by a single recoil. From 730 sequences with $\Delta t > 10$ ms it follows that about 0.15 chains could be random for $\Delta t = 0$–4 ms. Decay properties of these 25 R-SF chains occurring within $\Delta t = 0$–4 ms are given in Table I. These are separated into three groups. In the first group, three chains are given whose decay properties are in agreement with those expected for implantation and decay of ^{284}Fl. The next column contains sequences with properties, which fall out of the intervals chosen for ^{284}Fl. The last column includes short-lived SF nuclei with half-life of about 10 μs. Properties of all these decay chains except for two (Nos. 2 and 10) do not correspond to energy intervals assumed for ^{284}Fl. The possible origin of these events will be discussed in the following Sec. IV.

IV. DISCUSSION

In this experiment, three new decay chains of ^{285}Fl were observed, in addition to one chain identified at BGS in the ^{242}Pu(^{48}Ca,5n) reaction [7] and three chains detected at DGFRS in the ^{240}Pu(^{48}Ca,3n) reaction [1]. The decay properties of most nuclei in the new chains are in agreement with previous observations. However, in one case (chain 3 in Fig. 1) the decay time of ^{269}Sg exceeds the average lifetime determined for the five other observed events by a factor of 33. The measured decay properties of ^{285}Fl and descendant nuclides are shown in Fig. 3. The properties of nuclei observed in the third chain in Fig. 1 are shown by filled squares. Time intervals corresponding to a detection probability of about 97% of decays are shown by horizontal lines. These intervals were calculated for half-lives estimated from 7 (^{273}Hs—^{285}Fl) or 6 (^{265}Rf, ^{269}Sg) decays of nuclei (see Table II) and number of decays of 0.1 for time intervals below and above the given intervals. For all nuclei with the exception of ^{269}Sg, decays were observed within these intervals; only the decay time of ^{269}Sg in the third chain exceeds the upper limit calculated for all the six events. Despite the apparent difference in lifetimes for ^{269}Sg, the standard deviation of the logarithm of all the measured decay times is 1.54, which fits into the interval of 0.48–1.89 proposed in Ref. [8] for six exponentially decaying events. Thus, the available set of data does not provide a valid reason, which could confidently point out the inconsistency of the results obtained for ^{269}Sg in one of the seven decay chains. This behavior is not unexpected for statistically decaying nuclei.

However, one can see in Fig. 3 that decay times of nuclei in the considered chain are systematically lower than other lifetimes for all of the four isotopes ^{285}Fl, ^{281}Cn, ^{277}Ds, and

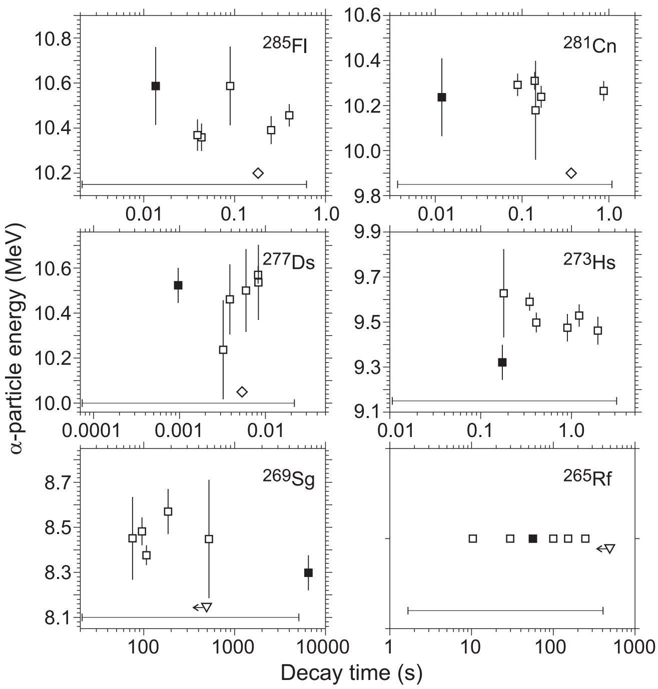

FIG. 3. Measured α-particle energies E_α (with error bars) vs. decay times of isotopes assigned to ^{285}Fl, ^{281}Cn, ^{277}Ds, ^{273}Hs, ^{269}Sg, and ^{265}Rf. For spontaneously fissioning ^{265}Rf, only decay times are shown. Decay properties of nuclei observed in the third decay chain in Fig. 1 are shown by filled squares. Time ranges for ^{269}Sg and ^{265}Rf in one chain with missing α decay of ^{269}Sg [1] are determined as intervals between decays of ^{273}Hs and ^{265}Rf and are shown by triangles with arrows (upper limits). Decay times for events with partially measured E_α values (full energy was not registered) are shown by diamonds on the bottom part of panels for ^{285}Fl [7], ^{281}Cn [1], and ^{277}Ds (this work). Time intervals corresponding to a detection probability of 97% of decays are shown by horizontal lines (see text).

^{273}Hs; the energies of α particles are comparable for the first three nuclides and somewhat lower for ^{273}Hs. The lifetime of ^{269}Sg in this one chain is larger than those for other six decays and its α-particle energy is lower, but not much, than those in the other five cases. The decay times of ^{265}Rf are comparable in all the chains. Such a difference in the decay properties of nuclei for one of the seven chains might imply

TABLE II. Decay properties of nuclei produced in this work and from Refs. [1,7].

Nuclide	Decay mode	Half-life[a]	E_α (MeV)[b]	Q_α (MeV)[b]
^{285}Fl	α	$0.10^{+0.06}_{-0.03}$ s	10.41 ± 0.05	10.56 ± 0.05
^{281}Cn	α	$0.18^{+0.10}_{-0.05}$ s	10.28 ± 0.04	10.43 ± 0.04
^{277}Ds	α	$3.5^{+2.1}_{-0.9}$ ms	10.55 ± 0.04	10.70 ± 0.04
^{273}Hs	α	$0.51^{+0.30}_{-0.14}$ s	9.51 ± 0.04	9.65 ± 0.04
^{269}Sg	α	14^{+10}_{-4} min	8.41 ± 0.04	8.54 ± 0.04
^{265}Rf	SF	$1.1^{+0.8}_{-0.3}$ min		

[a]Error bars correspond to 68% confidence level.
[b]The energy uncertainties correspond to the data with the best energy resolution.

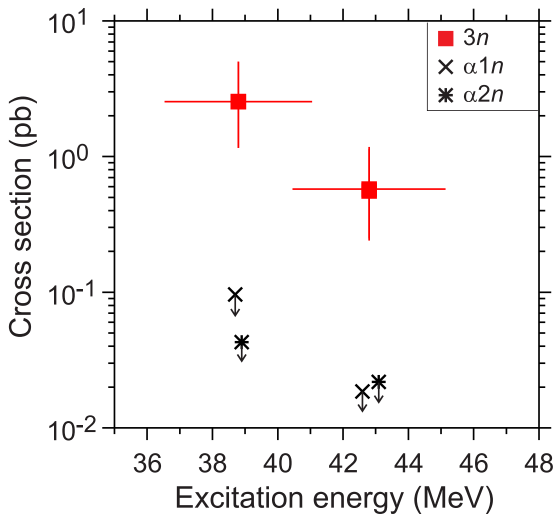

FIG. 4. Measured cross sections for the $3n$-evaporation channel for the ^{240}Pu + ^{48}Ca reaction (red squares). Vertical error bars correspond to total (statistical and systematic) uncertainties. Horizontal error bars represent the range of excitation energies populated at the given beam energy. Cross-section maxima for the αn and $\alpha 2n$ channels estimated with use of different models discussed in the text are shown by ×'s and asterisks (see insert).

transitions through their different energy levels. However, the existing data do not allow us to make a definitive conclusion. The average decay properties of nuclei observed in this work and in Refs. [1,7] are given in Table II assuming single half-lives for all of the nuclei. However, it should be noted that in this case, the half-life of ^{269}Sg is markedly increased compared with the value $T_{1/2} = 3.1^{+3.7}_{-1.1}$ min given in Ref. [1]. As mentioned above, the probability that an event with energy of 8.30 MeV is random and does not belong to the isotope ^{269}Sg seems to be quite small, which allows us to assign it to this isotope. In addition, in this chain, the decay time of ^{265}Rf is consistent with the values observed in the remaining six chains of this nucleus. In any case, the aggregate decay time of the isotopes ^{269}Sg and ^{265}Rf in the third chain differs from the average value determined from the other chains by a factor of almost 20. In this regard, taking into consideration that the discussed chain could represent decay through a different nuclear level, we chose to give here the decay properties for the states in ^{269}Sg that follow from the third chain taken alone (that is, $T_{1/2} = 75^{+360}_{-35}$ min, $E_\alpha = 8.30 \pm 0.08$ MeV) and from the remaining chains ($T_{1/2} = 2.3^{+1.7}_{-0.7}$ min, $E_\alpha = 8.43 \pm 0.04$ MeV).

The cross section of the ^{240}Pu(^{48}Ca,$3n$) reaction at 250 MeV beam energy was measured to be $0.58^{+0.60}_{-0.33}$ pb (for the summary beam dose collected in Ref. [1] and this work, see Fig. 4). The given error bars include statistical as well as systematic uncertainties. In comparison with data from Ref. [1], an increase of ^{48}Ca energy of 5 MeV resulted in a decrease of the cross section of the $3n$ channel by a factor of about 4–5, which is in agreement with expectations for this evaporation channel (see, e.g., Fig. 4 in Ref. [9]). In the same figure, it can be seen that the production cross sections of the $4n$-evaporation channel exceed those for the $3n$ channel at the excitation energy of the compound nucleus $E^* = 40$–45 MeV in most reactions where both these channels were observed. Only in reactions with relatively neutron-deficient ^{243}Am is the yield of the $3n$ channel larger at $E^* = 40$ MeV and with ^{245}Cm the products of the $4n$ channel were not observed. Note that ^{240}Pu is the most neutron-deficient isotope ($N - Z = 52$) of all of the target nuclides used in reactions with ^{48}Ca and where products of complete fusion were unambiguously identified, except for ^{237}Np with a $N - Z = 51$.

For the product of the $4n$ channel, the even-even isotope ^{284}Fl, one expects SF as a dominant decay mode with high confidence. It follows from the dependence of T_{SF} on the neutron number for ^{282,284}Cn and ^{286}Fl isotopes, as well as theoretical calculations [2] (see, e.g., Fig. 5 in Ref. [1]). In Ref. [1], using the measured half-life of two to four SF events, which we tentatively assigned to ^{284}Fl and comparing it with the partial α-decay half-life, which might be estimated from extrapolation of the α-decay energy Q_α systematics and relationship between T_α and Q_α, we estimated that ^{284}Fl could have about a 20% α-decay branch. α decay of ^{284}Fl was not observed in this experiment. Identifying new isotopes by SF decay properties is much more difficult compared with using α decay for several possible reasons. Among these are: the existence of long-lived SF activities in the detector from prior or current experiments and their random correlations with preceding ER-like events, the production of short-lived SF nuclides and SF isomers in transfer reactions and in reactions with emission of charged particles (pxn, αxn, etc.), relative yields of the latter may increase with increase of neutron deficit of target nuclei. All these sources of background may mimic decays of ^{284}Fl. Finally, the nonspecificity of fission complicates attribution of the observed SF to a particular nucleus.

The decay properties of the three nuclei in Table I (second column) are in agreement with those expected for ^{284}Fl. Their lifetimes are about 1 ms. The expected number of random ER-SF correlations due to longer-lived SF nuclides is rather low ($N_{\mathrm{ran}} < 0.15$, see above). Unfortunately, the energies of fission fragments in these chains are relatively low and cannot be an argument in favor of this assignment. The cross section corresponding to production of one ER-SF event of ^{284}Fl in this experiment is about 0.26 pb. Eight more chains were observed with comparable lifetimes but with characteristics somewhat different from what we expected for the products of complete fusion (third column in Table I). All or part of them could originate from SF isomers $^{240,244\mathrm{mf}}$Am and $^{242\mathrm{mf}}$Am, which decay with a half-life of about 1 ms and 14 ms, respectively [10]. Besides, several Pu and Am SF isomers with half-lives ranging within 1–73 μs ($^{237,239,241\mathrm{mf}}$Pu, $^{238,241,243,244,245,246\mathrm{mf}}$Am [10]) could also reach the detectors. Their half-lives are comparable with those shown in Fig. 2 at $\Delta t_{\mathrm{R-SF}} < 40$ μs and in the last column in Table I. For analysis of the origin of these R-SF chains one can consider data available for the ($\pm xn$)- and ($+p \pm xn$)-transfer reactions, which lead to Pu and Am SF isomers in the reaction with ^{240}Pu. In Fig. 5 (left panel), we show cross sections for production of Cf and Cm isotopes in the reactions of ^{86}Kr and ^{136}Xe heavy ions with ^{249}Cf and ^{248}Cm, respectively, vs. number of transferred neutrons ($\pm xn$). The cross sections for production

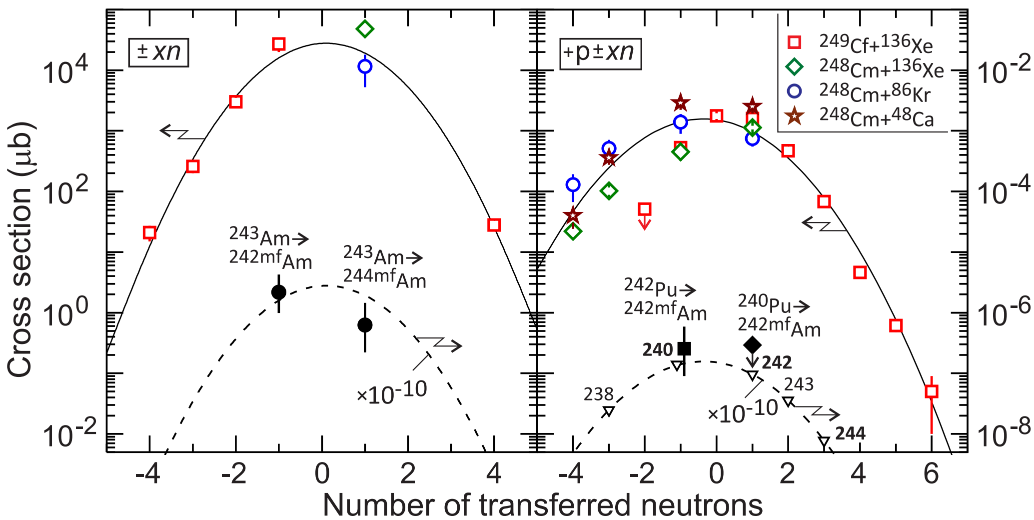

FIG. 5. Left: Cross sections for production of Cf isotopes in the ^{249}Cf + ^{136}Xe reaction [11] (red squares) and Cm isotopes in the reactions ^{248}Cm + ^{136}Xe [12] (green diamond) and ^{248}Cm + ^{86}Kr [12] (blue circle) vs. number of neutrons transferred to (positive values) or stripped from (negative ones) the target nuclei. Solid curve shows a Gaussian fit to these data. Cross sections (observed yield) measured at DGFRS for production of Am isomers with half-lives of 14 ms ($^{242\mathrm{mf}}$Am) and 1 ms (assigned to $^{244\mathrm{mf}}$Am) in the ^{243}Am + ^{48}Ca reaction at 248-MeV [13] are shown by black filled circles (right scale in μb). The dashed curve was obtained by shifting the upper fit curve down by a factor of 10^{10}. Note, production of $^{239\mathrm{mf}}$Pu and $^{241\mathrm{mf}}$Pu in the reaction with ^{240}Pu corresponds to the same number of transferred neutrons as that of $^{242\mathrm{mf}}$Am and $^{244\mathrm{mf}}$Am in the reaction with ^{243}Am. Right: The same as in the left panel but for production of Es and Bk isotopes in the reactions with ^{249}Cf and ^{248}Cm, respectively, vs. number of transferred neutrons ($+p \pm xn$). Data for the ^{248}Cm + ^{48}Ca reaction [14] are shown by brown stars. Production cross sections for $^{242\mathrm{mf}}$Am measured at DGFRS in the ^{242}Pu + ^{48}Ca reaction at 244–250 MeV [15] and in this experiment, are shown by a black filled square and diamond, respectively. Expected yields of Am SF isomers in the ^{240}Pu + ^{48}Ca reaction are shown by open triangles (see text). Atomic masses of isomers with $T_{1/2} > 0.1$ ms are given in bold.

of Es and Bk isotopes in the reactions of ^{48}Ca, ^{86}Kr, and ^{136}Xe with ^{249}Cf and ^{248}Cm ($+p \pm xn$), respectively, are shown in Fig. 5 (right panel). Projectile energies in these reactions correspond to about 1.07 times the Coulomb barrier [16], close to that in the ^{240}Pu + 250-MeV ^{48}Ca reaction. For conversion of these cross sections to yields of isomers, one should take into account the suppression factor of DGFRS for transfer-reaction products and isomeric ratio for SF isomers. Both these values are defined with large uncertainties.

However, the product of these values may be estimated from the ^{243}Am + ^{48}Ca [13] and ^{242}Pu + ^{48}Ca [15] experiments where several R-SF chains were observed and assigned to Am isomers. The measured yields of 14-ms ($^{242\mathrm{mf}}$Am) and 1-ms (assigned to $^{244\mathrm{mf}}$Am) activities in the first reaction at the excitation energy of 40 MeV are shown in the left panel in Fig. 5. The curve fitting the cross sections of the ($\pm xn$)-transfer reactions with ^{248}Cm and ^{249}Cf targets was scaled down by a factor of 10^{10} (dashed curve in Fig. 5). To obtain this somewhat arbitrary factor we assumed reasonable values for the isomeric ratio (3.3×10^{-4} [17]) and the DGFRS suppression factor for transfer-reaction products (3.3×10^{6}, see, e.g., Ref. [18]). The observed yields of $^{242,244\mathrm{mf}}$Am are close to this reduced yield curve. Note, these Am isomers are produced in the same transfer reaction as $^{239\mathrm{mf}}$Pu and $^{241\mathrm{mf}}$Pu in the ^{240}Pu + ^{48}Ca reaction. Similarly, the yield of $^{242\mathrm{mf}}$Am was measured in the ^{242}Pu + ^{48}Ca reaction at 244–250 MeV projectiles [15]. Finally, the upper limit of the yield of $^{242\mathrm{mf}}$Am in the ^{240}Pu + ^{48}Ca reaction can be estimated from nonobservation of 14-ms activity within the time interval of 3.6–23 ms (see Fig. 2) where more than 50% of its decays should be registered. Again, the yields of $^{240,242\mathrm{mf}}$Am agree with the curve obtained by shifting the fitting curve for the ($+p \pm xn$)-transfer reactions shown in Fig. 5 (right panel) by the same factor of 10^{10}.

In further analysis of the results, we assume that both the suppression factors of DGFRS for products of the low-nucleon transfer reactions and isomeric ratios for different nuclides produced in different reactions are close. However, the suppression factor can depend on target thickness, projectile energy, and separator settings; at the same time, the isomeric ratios could differ for the particular isomer, reaction type, projectile energy, etc. Nevertheless, the summary yield of SF isomers with half-lives of $\sim$1 μs to 73 μs expected from reduced curves in Fig. 5 could exceed the yield of the 1-ms $^{240,242,244\mathrm{mf}}$Am by a factor of about 17. If so, taking into account this factor and the number of R-SF events with $T_{1/2} \approx 10$ μs, one could expect observation of one decay of $^{240,244\mathrm{mf}}$Am.

Another possible source of the 1-ms SF activity could be ^{282}Cn, the product of the $\alpha 2n$ reaction with ^{240}Pu. In this regard, the R-α-SF chain observed in this experiment should be discussed first. The decay properties of this chain are similar to the decay of ^{283}Cn ($E_\alpha = 9.53$, 9.33, 8.94 MeV [9,18,19]; $T_\alpha = 4.2^{+1.1}_{-0.7}$ s [9,18], $4.48^{+0.98}_{-0.68}$ s [19]) followed by SF of ^{279}Ds (SF branch $b_{\mathrm{SF}} = 90\%$ [9,18], 85% [19]; $T_{\mathrm{SF}} = 0.21 \pm 0.04$ s [9,18], $0.290^{+0.069}_{-0.047}$ s [19]). The chain in question could start from ^{287}Fl ($E_\alpha = 10.03$ MeV [9,18,19]; $T_\alpha = 0.48^{+0.14}_{-0.09}$ s [9,18], $0.54^{+0.17}_{-0.10}$ s [19]), the product of the $1n$ channel with ^{240}Pu, whose α particle was not registered (see above). However, the products of the $1n$ channel were not observed in other ^{48}Ca-induced reactions with various actinide target nuclei [9,18]. One expects an even lower probability for this $1n$-reaction channel at such high excitation energy of the compound nucleus ($E^* = 42.8$ MeV). But, despite the fact that the content of ^{242}Pu impurity in the JINR target material seems to be low (2.0%), the detection of one R-α-SF chain results in a production cross section of ^{287}Fl in the ^{242}Pu + ^{48}Ca reaction of about 10^{+25}_{-9} pb, which does not contradict values measured for this reaction [15]. Thus, this chain could be caused by ^{287}Fl, the product of the $3n$-evaporation channel of the reaction with ^{242}Pu impurity in the target.

Nevertheless, the potential αn channel for the ^{240}Pu + ^{48}Ca reaction leads directly to ^{283}Cn. The products of the αxn-reaction channels were never clearly observed in previous studies of the reactions of ^{48}Ca with actinide target nuclei. However, the lower mass number of the compound nuclei could lead to increased competitiveness of these channels compared to the xn channel (see, e.g., Ref. [20]). Unfortunately, existing theoretical models that describe fusion of heavy nuclei and further deexcitation of the compound nucleus are not sufficient to provide accurate quantitative results. To simplify the procedure, we omitted calculations of the first two steps of fusion-evaporation process—capture of interacting nuclei and following stage of formation of compound nuclei—and calculated only survival probabilities of the excited nuclei with respect to different channels. Then, using the calculated ratios between probabilities of the αxn and $3n$ channels and the measured cross sections of the $3n$ channel, we could estimate the cross section of the αxn channels.

In calculations of the ratios between the αxn and $3n$ channels we used three versions of a statistical model. One of them is the NRV statistical code of decay of excited nuclei [21,22]. Within this model, the fission barriers are calculated as a difference between the finite-range droplet barriers [23] and the shell corrections to the ground-state masses. These masses, necessary for calculating the particle binding energies, as well as the corresponding shell corrections are taken from Ref. [24]. In the second approach, calculations are performed within a framework of the statistical model realized with the HIVAP code [25]. The empirical masses [26] together with the liquid-drop (LD) finite-range ones [27] (for the nuclei not presented in Table [26]) are used for the calculations of the excitation and separation energies. Rotating LD fission barriers [28] are used in calculations together with shell correction energies (the difference between empirical and LD masses). Finally, in the third approach, the formation of the CN is described within a version of the dinuclear system model (see Ref. [29] and references therein). The deexcitation of the CN is treated with the statistical model using the level densities from the Fermi-gas model. The neutron, proton, and α-particle binding energies, the nuclear mass excesses of superheavy nuclei, and the ground-state microscopic corrections are taken from Ref. [27]. Within these three approaches, a satisfactory agreement was achieved in predicting and/or reproducing the (^{48}Ca,xn) excitation functions measured in the reactions with actinide target nuclei [29–31].

The ratios between probabilities of the αxn and $3n$ channels at $E^* = 43$ MeV vary within 0.001–0.03 and 0.01–0.04 for the $\alpha 1n$ and $\alpha 2n$ channels, respectively. The estimated cross-section maxima for the $\alpha 1n$ and $\alpha 2n$ channels, namely, ^{283}Cn and ^{282}Cn, are shown in Fig. 4. Note, the yields of the αxn-reaction products are expected to be even lower due to reduced transmission efficiency of DGFRS for products of the αxn channels compared with that for the xn channels which was estimated to be about a factor of 4 [32,33]. This value follows from a Monte Carlo code [34] that allows simulation of angular and energy distributions of ERs at the exit from the target. Thus, it provides the input data for an ion-optical program [35] designed for tuning the separator and estimating the transmission and final yield of the reaction products in question. We also used a different Monte Carlo approach for calculating angular and energy distributions of ERs and their transmission though the DGFRS's diaphragm [33]. In this approach, the HIVAP code was used for calculating initial distributions inside a target and the TRIM code for the simulation of transmission of ERs through a target layer. These calculations gave essentially the same values of the suppression factors. The yield of the $\alpha 1n$ channel is expected to be lower than that of the $3n$ channel by a factor of 120–4000. Thus, assignment of the R-α-SF chain to the product of the $\alpha 1n$ channel does not look probable. Nevertheless, none of the three discussed sources of the R-α-SF chain can be excluded with certainty. Several factors prevent us from making definite conclusions; these are: observation of a single event only, somewhat long R-α time interval and large uncertainty of α-particle energy assigned to ^{283}Cn, which raises some concerns in identifying the parent nucleus, and possible uncertainties in the calculation of the DGFRS transmission for the αxn channels and cross-section ratios of αxn and xn channels.

Similarly, the product of the $\alpha 2n$-reaction channel, ^{282}Cn (SF, $T_{1/2} = 0.91^{+0.33}_{-0.19}$ ms [9,18], $0.96^{+0.35}_{-0.20}$ ms [19]), could contribute to the 1-ms SF activity (see Fig. 2). However, taking into account predictions of the discussed models and the reduced transmission efficiency of DGFRS for the αxn-reaction products, the yield of ^{282}Cn at $E^* = 43$ MeV is expected to be lower by more than two orders of magnitude compared with that for the $3n$ channel. If contrary to the calculations, the R-α-SF chain originates from the $\alpha 1n$ channel, the observation of several decays of ^{282}Cn cannot be excluded.

In summary, three new decay chains of ^{285}Fl were observed in the ^{240}Pu(^{48}Ca,$3n$) reaction at 250-MeV ^{48}Ca energy. The decay properties of the observed nuclei are mostly in agreement with those measured in other chains, namely the one identified at the BGS in the ^{242}Pu(^{48}Ca,$5n$) reaction [7] and three at the DGFRS in the ^{240}Pu(^{48}Ca,$3n$) reaction at lower energy [1]. The lifetime of ^{269}Sg observed in one chain exceeds that derived from other five decays by a factor of 33, which might indicate the observation of transitions through different levels in ^{285}Fl and descendants. The cross section of the ^{240}Pu(^{48}Ca,$3n$)^{285}Fl reaction was measured to be $0.58^{+0.60}_{-0.33}$ pb, which is lower by a factor of about 4–5 than the value measured at 245-MeV ^{48}Ca energy [1] and is in agreement with expectations for the $3n$-evaporation channel.

One R-α-SF chain looks similar to the decay of ^{283}Cn followed by SF of ^{279}Ds. The chain could start in fact from ^{287}Fl, whose α particle was not registered, and be a product of the $1n$ channel of the ^{240}Pu + ^{48}Ca reaction or originate from the $3n$ channel of the reaction of ^{48}Ca with ^{242}Pu impurity in the target. The $\alpha 1n$-reaction channel leading directly to ^{283}Cn cannot be completely excluded as well. Of the above three possible sources of this chain, the reaction with ^{242}Pu impurity in the target appears to be the most reasonable.

More than 20 short-lived SF nuclei with lifetimes of about 10 μs and 1 ms were observed. Usually, identification of the spontaneously fissioning nucleus is not an easy task. Several sources of these activities were considered, namely, products of transfer reactions—spontaneously fissioning isomers $^{237,239,241\text{mf}}$Pu and $^{238,241,243,244,245,246\text{mf}}$Am ($T_{\text{SF}} =$ 1–73 μs) and $^{240,242,244\text{mf}}$Am ($T_{\text{SF}} = 1$ ms and 14 ms) as well as products of the $\alpha 2n$ channel, ^{282}Cn ($T_{\text{SF}} = 1$ ms), and $4n$-evaporation product, ^{284}Fl. Comparison of the cross sections of several transfer reactions, which lead to products of the transfer/capture of neutrons solely ($\pm$xn) or together with transfer of proton to the target nucleus ($+p \pm xn$) with observed yields of SF activities was carried out, assuming similar suppression factors and isomeric ratios for discussed reaction products. From this analysis it follows that the most probable sources of the ~ 10 μs activity are isotopes $^{239\text{mf}}$Pu ($T_{\text{SF}} = 7.5$ μs) and $^{241\text{mf}}$Pu ($T_{\text{SF}} = 20.5$ μs) (see, e.g., 14 events in the last column in Table I). Their yields are expected to be larger than the total yield of $^{240,242,244\text{mf}}$Am by a factor of about 17. Correspondingly, one could expect observation of about one decay of $^{240-244\text{mf}}$Am. The products of the αxn-reaction channels were not observed with certainty in previous studies of the reactions of U-Cf isotopes with ^{48}Ca, which is in agreement with combined analysis of the results of this experiment and calculations [21,22,25,29]. However, if the detected R-α-SF chain originates from ^{283}Cn, a potential product of the $\alpha 1n$ channel, then one may expect that several events of the product of the $\alpha 2n$ channel, ^{282}Cn, could contribute to the 1 ms activity, e.g., those shown in column 3 in Table I. In addition, observation of several decays of ^{284}Fl (e.g., see column 2 in Table I) cannot be excluded as well. The observed decay properties would be in agreement with empirical systematics of the half-lives of even-even nuclides ^{282,284}Cn and ^{286}Fl and predictions for T_{SF} of the isotopes of Ds-Og [2]. The number of observed events also would not contradict to the measured ratios between cross sections of the $3n$ and $4n$-evaporation channels for the reactions with heavier Pu isotopes at the excitation energy of compound nucleus $E^* =$ 40–45 MeV [9,18]. All of these considerations are valid for the results obtained in the first experiment with ^{239,240}Pu targets [1]. Here we should note that the unambiguous identification of ^{284}Fl still requires further studies, e.g., detection of the α-decay mode of ^{284}Fl, preferably with highly purified ^{240}Pu target material, or observation of ^{284}Fl as an α-decay product of the parent nucleus ^{288}Lv. However, taking into account the presumably low α-decay branch of ^{284}Fl and low production cross section of ^{288}Lv in any realizable reaction, these measurements call for performing experiments with noticeably higher sensitivity.

ACKNOWLEDGMENTS

We would like to express our gratitude to the personnel of the U400 cyclotron and the associates of the ion-source group for obtaining intense ^{48}Ca beams. The ^{240}Pu used in this research was partially supplied by the United States Department of Energy Office of Science by the Isotope Development and Production for Research and Applications Program in the Office of Nuclear Physics. These studies were supported by the Russian Foundation for Basic Research, including recent Grants No. 13-02-12052 and No. 16-52-55002. Research at ORNL was supported by the U.S. DOE Office of Nuclear Physics under DOE Contract No. DE-AC05-00OR22725 with UT Battelle, LLC. Research at LLNL was supported by LDRD Program Project No. 08-ERD-030, under DOE Contract No. DE-AC52-07NA27344 with Lawrence Livermore National Security, LLC. This work was also supported by the U.S. DOE through Grant No. DE-FG-05-88ER40407 (Vanderbilt University) and by the National Natural Science Foundation of China (Grant No. 11661131003).

[1] V. K. Utyonkov, N. T. Brewer, Yu. Ts. Oganessian, K. P. Rykaczewski, F. Sh. Abdullin, S. N. Dmitriev, R. K. Grzywacz, M. G. Itkis, K. Miernik, A. N. Polyakov, J. B. Roberto, R. N. Sagaidak, I. V. Shirokovsky, M. V. Shumeiko, Yu. S. Tsyganov, A. A. Voinov, V. G. Subbotin, A. M. Sukhov, A. V. Sabel'nikov, G. K. Vostokin, J. H. Hamilton, M. A. Stoyer, and S. Y. Strauss, Phys. Rev. C **92**, 034609 (2015).
[2] R. Smolańczuk, J. Skalski, and A. Sobiczewski, Phys. Rev. C **52**, 1871 (1995).
[3] Meng Wang, G. Audi, F. G. Kondev, W. J. Huang, S. Naimi, and Xing Xu, Chin. Phys. **41**, 030003 (2017).
[4] W. D. Myers and W. J. Swiatecki, Nucl. Phys. A **601**, 141 (1996).
[5] N. T. Brewer *et al.* (unpublished).
[6] K.-H. Schmidt, C.-C. Sahm, K. Pielenz, and H.-G. Clerc, Z. Phys. A **316**, 19 (1984).
[7] P. A. Ellison *et al.*, Phys. Rev. Lett. **105**, 182701 (2010).
[8] K.-H. Schmidt, Eur. Phys. J. A **8**, 141 (2000).
[9] Yu. Ts. Oganessian and V. K. Utyonkov, Nucl. Phys. A **944**, 62 (2015).
[10] G. Audi, F. G. Kondev, Meng Wang, W. J. Huang, and S. Naimi, Chin. Phys. **41**, 030001 (2017).
[11] K. E. Gregorich, K. J. Moody, D. Lee, W. K. Kot, R. B. Welch, P. A. Wilmarth, and G. T. Seaborg, Phys. Rev. C **35**, 2117 (1987).
[12] K. J. Moody, D. Lee, R. B. Welch, K. E. Gregorich, G. T. Seaborg, R. W. Lougheed, and E. K. Hulet, Phys. Rev. C **33**, 1315 (1986).
[13] Yu. Ts. Oganessian *et al.*, Phys. Rev. C **87**, 014302 (2013).
[14] D. C. Hoffman *et al.*, Phys. Rev. C **31**, 1763 (1985).
[15] Yu. Ts. Oganessian *et al.*, Phys. Rev. C **70**, 064609 (2004).
[16] R. Bass, in *Proceedings of the Symposium on Deep Inelastic and Fusion Reactions with Heavy Ions*, edited by W. von Oertzen, Lecture Notes in Physics, Vol. 117 (Springer-Verlag, Berlin, 1980), p. 281.

[17] Yu. Ts. Oganessian, Yu. V. Lobanov, M. Hussonnois, Yu. P. Kharitonov, B. Gorski, O. Constantinescu, A. G. Popeko, H. Bruchertseifer, R. N. Sagaidak, S. P. Tretyakova, G. V. Buklanov, A. V. Rykhlyuk, G. G. Gulbekyan, A. A. Pleve, G. N. Ivanov, and V. M. Plotko, in *Proceedings of the International School of Physics "Enrico Fermi", Trends in Nuclear Physics*, edited by P. Kienle, R. A. Ricci, and A. Rubbino, 23 June–3 July, 1987, Varenna, Italy (CIII Corso, Soc. Italiana di Fisica, Bologna, 1989), pp. 258–281.

[18] Yu. Ts. Oganessian and V. K. Utyonkov, Rep. Prog. Phys. **78**, 036301 (2015).

[19] S. Hofmann *et al.*, Eur. Phys. J. A **52**, 180 (2016).

[20] D. Vermeulen, H.-G. Clerc, C.-C. Sahm, K.-H. Schmidt, J. G. Keller, G. Münzenberg, and W. Reisdorf, Z. Phys. A **318**, 157 (1984).

[21] V. I. Zagrebaev, A. S. Denikin, A. V. Karpov, A. P. Alekseev, M. A. Naumenko, V. A. Rachkov, V. V. Samarin, and V. V. Saiko, NRV web knowledge base on low-energy nuclear physics, http://nrv.jinr.ru/

[22] A. V. Karpov, A. S. Denikin, A. P. Alekseev, V. I. Zagrebaev, V. A. Rachkov, M. A. Naumenko, and V. V. Saiko, Phys. At. Nucl. **79**, 749 (2016); A. V. Karpov, A. S. Denikin, M. A. Naumenko, A. P. Alekseev, V. A. Rachkov, V. V. Samarin, V. V. Saiko, V. I. Zagrebaev, Nucl. Instrum. Methods Phys. Res., Sect. A **859**, 112 (2017).

[23] A. J. Sierk, Phys. Rev. C **33**, 2039 (1986).

[24] P. Möller, A. J. Sierk, T. Ichikawa, and H. Sagawa, At. Data Nucl. Data Tables **109-110**, 1 (2016).

[25] W. Reisdorf, Z. Phys. A **300**, 227 (1981); W. Reisdorf and M. Schädel, *ibid.* **343**, 47 (1992).

[26] G. Audi, A. H. Wapstra, and C. Thibault, Nucl. Phys. A **729**, 337 (2003).

[27] P. Möller, J. R. Nix, W. D. Myers, and W. J. Swiatecki, At. Data Nucl. Data Tables **59**, 185 (1995).

[28] S. Cohen, F. Plasil, and W. J. Swiatecki, Ann. Phys. (N.Y.) **82**, 557 (1974).

[29] Juhee Hong, G. G. Adamian, N. V. Antonenko, Phys. Lett. B **764**, 42 (2017); G. G. Adamian (private communication).

[30] V. I. Zagrebaev and W. Greiner, Nucl. Phys. A **944**, 257 (2015).

[31] R. N. Sagaidak, EPJ Web Conf. **21**, 06001 (2012); TAN11 presentation, Sochi, 2011 (unpublished).

[32] A. G. Popeko, Nucl. Instrum. Methods Phys. Res., Sect. B **376**, 144 (2016).

[33] R. N. Sagaidak, V. K. Utyonkov, and F. Scarlassara, Nucl. Instrum. Methods Phys. Res., Sect. A **700**, 111 (2013).

[34] A. G. Popeko, O. N. Malyshev, R. N. Sagaidak, and A. V. Yeremin, Nucl. Instrum. Methods Phys. Res., Sect. B **126**, 294 (1997).

[35] A. G. Popeko, O. N. Malyshev, A. V. Yeremin, and S. Hofmann, Nucl. Instr. Methods Phys. Res., Sect. A **427**, 166 (1999).